**OXYGEN FUGACITY AT HIGH PRESSURE: EQUATIONS OF STATE OF METAL-OXIDE PAIRS.** A. J. Campbell[1], L. Danielson[2], K. Righter[2], Y. Wang[3], and G. Davidson[1], [1]Dept. of Geology, University of Maryland, College Park, MD 20742 (ajc@umd.edu); [2]Johnson Space Center, NASA, Houston, TX 77058; [3]Center for Advanced Radiation Sources, University of Chicago, Argonne, IL 60439.

**Introduction:** Oxygen fugacity ($fO_2$) varies by orders of magnitude in nature, and can induce profound changes in the chemical state of a substance, and also in the chemical equilibrium of multicomponent systems. One prominent area in high pressure geochemistry, in which $fO_2$ is widely recognized as a principal controlling factor, is that of metal-silicate partitioning of siderophile trace elements (e.g., [1]). Numerous experiments have shown that high pressures and temperatures can significantly affect metal/silicate partitioning of siderophile and moderately siderophile elements. Parameterization of these experimental results over P, T, X, and $fO_2$ can allow the observed siderophile element composition of the mantle to be associated with particular thermodynamic conditions [2]. However, this is best done only if quantitative control exists over each thermodynamic variable relevant to the experiments. The $fO_2$ values for many of these partitioning experiments were determined relative to a particular metal-oxide buffer (e.g., Fe-FeO (IW), Ni-NiO (NNO), Co-CoO, Re-$ReO_2$ (RRO)), but the parameterization of all experimental results is weakened by the fact that the pressure-induced relative changes between these buffer systems are imprecisely known.

For the general metal-oxide reaction

$$M + (x/2)\ O_2 = MO_x,$$

the $fO_2$ is related to the Gibbs energies (G) by

$$(x/2)\ RT \ln fO_2 = G(MO_x) - G(M).$$

The pressure effect on this buffer is in the G terms. Along each isotherm, $dG = VdP$. Extension of the 1-bar $fO_2$ buffers to high pressure, high-temperature conditions thus depends on the equations of state of each phase, but some of the relevant equations of state are poorly known. Furthermore, comparing $\Delta V$ between two independently measured equations of state compounds the errors associated with them. In this study we measure metal-oxide buffer pairs simultaneously using synchrotron radiation at high pressure and temperature. This minimizes systematic biases that might appear between studies, improving the precision of the $\Delta V$ data used to determine the high pressure $fO_2$ buffers.

**Experimental:** High purity (>99.9%, from Alfa Aesar) and fine grained (< 5 μm) mixtures of Ni-NiO, Fe-$Fe_{1-x}O$ and Re-$ReO_2$ were mixed with NaCl, which was used as a pressure standard during the runs. These mixtures were then loaded into a boron nitride capsule which was machined to fit within a specially developed beamline version of a 14/8 assembly developed by the COMPRES multi-anvil assembly initiative [3]. The octahedron is extrusion molded $MgAl_2O_4$ (spinel) which, together with the BN capsule, graphite furnace, and an outer forsterite sleeve, is more transparent to x-rays than standard assemblies. More standard features of the assembly are a Type C W-Re thermocouple, TZM sleeves around the alumina thermocouple sheaths, pyrophyllite gaskets, and teflon tape and laser-cut paper on opposing cubes. 8 mm truncated edge lengths were ground into the corners of 25.4 mm Fansteel tungsten carbide cubes (F equivalent).

The octahedral assemblies were loaded into the multi-anvil press at GSECARS, Sector 13 of the Advanced Photon Source [4], and pressurized for in situ, high-P,T X-ray diffraction using synchrotron radiation. In the experiments reported here, maximum pressures were limited to ~10 GPa, to preserve the experimental tooling, and maximum temperatures were limited to 1000 ºC to avoid conversion of the graphite heaters to diamond.

Diffraction patterns were collected at a series of P,T points for each sample; in this way the molar volume of the metal and metal oxide in each buffer pair were determined under identical P,T conditions, allowing intercalibration of their equations of state. Temperature was cycled at each of several hydraulic load settings. The pressure varied slightly with the changing temperature, because of competing effects of gasket softening and thermal pressure.

Energy dispersive x-ray diffraction was used, with a fixed diffraction angle (2θ) angle of ~6º. Exposure times were 300 s, and diffraction peak positions were determined by gaussian peak fitting after background subtraction. Lattice parameters were obtained from linear regressions to the measured d-spacings and their assigned Miller indices.

**Results:** An important observation is that no structural transitions were observed in NiO or $ReO_2$, and no intermediate phases appeared in the Ni-NiO or Re-$ReO_2$ experiments. The absence of any such transitions allows these $fO_2$ buffers to be calculated at high pressures in a straightforward manner, using the thermoelastic data on Ni, Re, and their oxides. The

extensive data processing is underway, and detailed results from only the Re-$ReO_2$ system are presented in this abstract.

To our knowledge, these are the first reported data on the compression or thermal expansion of $ReO_2$. In the Re-$ReO_2$ measurements, the NaCl peaks were very weak and overlapped significantly with those of other phases, so the equation of state of Re [5] was used as the pressure calibration. The bulk modulus, $K_T$, of $ReO_2$ (orthorhombic phase) was determined to be 180±4 GPa, based on a fit of the high-P,T data to a thermal equation of state [6]. $ReO_2$ is twice as compressible as Re ($K_T$=360 GPa [6]).

The volume difference between $ReO_2$ and Re ($\Delta V_{RRO}$) is shown as a function of pressure and temperature in Figure 1. A fit to a simple expression:

$$\Delta V_{RRO} = A*P + B*\Delta T$$

is also shown in the figure. The r.m.s. value for this fit is 0.02 $cm^3$/mol, or 0.2%. The use of a higher order expression did not significantly improve the fit.

These data can be used to evaluate the ΔG of the Re-$ReO_2$ buffer at high pressures, by integrating the $\int\Delta V_{RRO}$ dP term in the equation above. This has been done to construct Figure 2, which shows the effect of 10 GPa pressure on the IW and RRO oxygen fugacity buffers. The pressure effect on the IW buffer was calculated on the basis of published equations of state of Fe and $Fe_{1-x}O$, both of which are well-studied (e.g., [7]), but which may be subject to small relative biases, as discussed above. The pressure effect on the RRO buffer was calculated on the basis of our XRD results and the equations above. The pressure effects on the IW and RRO buffers are remarkably similar. The difference between the two $(\log(fO_2)_{RRO}-\log(fO_2)_{IW})$ remains nearly the same (within 0.1 log units) even when extrapolated to 20 GPa, over 1000≤T≤2200 K. This is a useful result, because it indicates that relative $fO_2$ values determined in previous high pressure experiments using either the IW or RRO buffers are readily comparable, and not subject to a significant systematic error from different pressure effects on the two buffers. This is not a general result appropriate to all $fO_2$ buffers, but a coincidence in high-pressure effects on the IW and RRO buffers.

**References:** [1] Righter K. and Drake M. J. (2003) In *The Mantle and Core* (Ed. R. Carlson), Elsevier, pp. 425-449. [2] Righter K. et al. (1997) *Phys. Earth Planet. Int., 100*, 115-34; Li J. and Agee C. B. (2001) *Geochim. Cosmochim. Acta, 65*, 1821-32; Chabot N. L. et al. (2005) *Geochim. Cosmochim. Acta, 69*, 2141-2151. [3] Leinenweber K. and Tyburczy J. (2005) In *Year 3 Annual Report of COMPRES* (http://www.compres.stonybrook.edu-/Publications/index.html), pp. 72-81. [4] Uchida T. et al. (2002) *J. Phys. Condens. Matter, 14,* 11517-11523. [5] Zha et al. (2004) Rev. Sci. Instrum., 75, 2409-2418.[6] Anderson et al. (1989) J. Ap. Phys., 65, 1534. [7] Fei Y. (1996) In *Mineral Spectroscopy* (Eds. M. D. Dyar et al.), Geochemical Soc., pp. 243-254; Uchida T. et al. (2001) *J. Geophys. Res., 106*, 21799-21810.

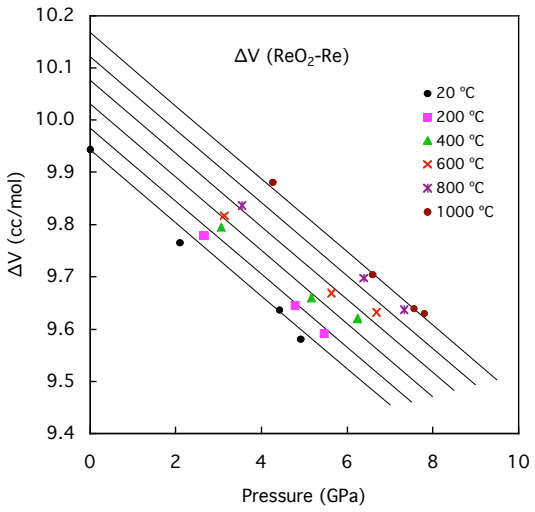


Figure 1. Effect of pressure and temperature on $\Delta V_{RRO}$.

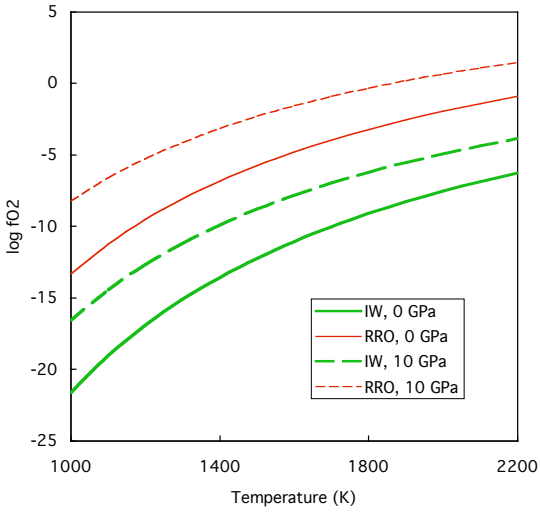


Figure 2. Effect of pressure on the IW [7] and RRO [this study] buffers.